Electromagnetic Boundary Conditions

William Bidle and Beatrice Liang-Gilman
Department of Physics and Astronomy, Rutgers University
(Dated: 12 October 2020)

Abstract In this report, we study the different phenomena of laser light at an optical interface, and experimentally validate Fresnel's equations for the case of a non-conducting, nonmagnetic transparent medium. By utilizing Snell's Law, we find the unknown indices of refraction for two semicircular materials, as well as determine their critical angles. Brewster's angle is similarly found by analyzing the transmitted and reflected beam powers for a specific beam polarization with respect to the medium.

I. INTRODUCTION AND THEORY

The electromagnetic boundary conditions, the Fresnel Coefficients, Snell's Law, and Brewster's angle can all be derived from Maxwell's equations in integral form:

$$\int \vec{E} \cdot d\vec{a} = \frac{q_{enclosed}}{\varepsilon_0}$$
$$\int \vec{B} \cdot d\vec{a} = 0$$
$$\int \vec{E} \cdot d\vec{l} = \iint -\frac{\partial \vec{B}}{\partial t} \cdot d\vec{a}$$
$$\int \vec{B} \cdot d\vec{l} = \mu_0 I_{enclosed} + \mu_0 \varepsilon_0 \iint \frac{\partial \vec{E}}{\partial t} \cdot d\vec{a}$$

Where $q_{enclosed}$ is the charge enclosed, $I_{enclosed}$ is the current enclosed, and $\vec{E}$ and $\vec{B}$ are the electric and magnetic fields respectively. A full derivation of the boundary conditions between two media will be omitted (see [1] or [2] for a full treatment), however the results with no enclosed charge or current are as follows:

$$\varepsilon_2 \vec{E}_2^{\perp} - \varepsilon_1 \vec{E}_1^{\perp} = 0$$
$$\vec{B}_2^{\perp} - \vec{B}_1^{\perp} = 0$$
$$\vec{E}_2^{\parallel} - \vec{E}_1^{\parallel} = 0$$
$$\mu_2{}^{-1} \vec{B}_2^{\parallel} - \mu_1{}^{-1} \vec{B}_1^{\parallel} = 0$$

Where the superscripts $\perp$ and $\parallel$ represent the components of the fields perpendicular and parallel to the surfaces respectively, and the subscripts 1 and 2 are for the mediums the fields are leaving and entering respectively. These equations can then be used to study the properties of light at a boundary, and it is straightforward to apply them to monochromatic E and B plane waves (again see [1] or [2] for a full derivation), and arrive at the results for the behavior of light passing from one medium to another, also known as Snell's Law:

$$n_1 \sin(\theta_1) = n_2 \sin(\theta_2)$$

Where θ_1 is the incident angle, θ_2 is the transmitted angle, n_1 is the index of refraction of the first material, and n_2 is the index of refraction of the second material. The important thing about this equation is that it is independent of polarization of the incident light and doesn't rely on the transverse nature of light (i.e. Snell's law can work for longitudinal waves). The relationship comes from relating the wave numbers and velocities of the incident, reflected, and transmitted light, and noting that the frequency of light in each medium must be the same. This equation can then be used to calculate the index of refraction for samples of interest by measuring the incident and transmitted angles[1].

Having calculated the index of refraction of the unknown material with Snell's Law, it is then straightforward to determine the critical angle. The critical angle of any material is a special condition for light going from a denser to less dense medium, where the transmitted light completely disappears as it makes an angle of 90° from the normal. Incident angles greater than the critical angle then undergo total internal reflection at the boundary and all of the incident light is reflected. By substituting $\theta_2 = 90^{\circ}$ into Snell's Law and solving for $\theta_1 = \theta_c$:

$$\theta_c = \arcsin\left(\frac{n_2}{n_1}\right)$$

The last and final phenomena of note that comes from the boundary conditions is Brewster's angle and it can be derived from the Fresnel Equations (again see [1] or [**Error! Bookmark not defined.**] for a full derivation):

[1] At least one of the indices of refraction need to be known to use the equation. In most cases n_1 or n_2 is the index of refraction of air equal to 1.

$$R_S = \frac{n_1\cos(\theta_1) - n_2\sqrt{1-\left(\frac{n_1}{n_2}\sin(\theta_1)\right)^2}}{n_1\cos(\theta_1) + n_2\sqrt{1-\left(\frac{n_1}{n_2}\sin(\theta_1)\right)^2}}$$

$$T_S = \frac{2n_1\cos(\theta_1)}{n_1\cos(\theta_1) + n_2\sqrt{1-\left(\frac{n_1}{n_2}\sin(\theta_1)\right)^2}}$$

$$R_P = \frac{n_1\sqrt{1-\left(\frac{n_1}{n_2}\sin(\theta_1)\right)^2} - n_2\cos(\theta_1)}{n_1\sqrt{1-\left(\frac{n_1}{n_2}\sin(\theta_1)\right)^2} + n_2\cos(\theta_1)}$$

$$T_P = \frac{2n_2\sqrt{1-\left(\frac{n_1}{n_2}\sin(\theta_1)\right)^2}}{n_1\cos(\theta_1) + n_2\sqrt{1-\left(\frac{n_1}{n_2}\sin(\theta_1)\right)^2}}$$

Where R and T are the reflected and transmitted amplitudes of light at the interface of two media respectively, and the subscripts S and P correspond to perpendicular (0°) and parallel (90°) polarizations respectively. In looking for an incident angle where there is zero reflected light (i.e. setting R_S and R_P equal to zero), we find that only the perpendicular case yields a solution, and that solution is the Brewster's angle:

$$\theta_B = \arctan\left(\frac{n_2}{n_1}\right)$$

Note that since this equation uses arctangent, it works for both orientations of the material (i.e. light going from the material to air and light going from air to the material).

The squares of the above Fresnel Equations, called the reflectance and transmittance coefficients, represent the respective intensities of the beam, which are useful in creating theoretical curves to compare with experimental data taken in this lab. These coefficients are experimentally determined using the following equations where j refers to either P or S polarization:

$$r_j = R_j^2 = \frac{I_r}{I_i}$$

$$t_j = T_j^2 = \frac{I_t}{I_i}$$

II. APPARATUS AND PROCEDURE

The experimental apparatus can be seen in Figure 1 below. A 2 mW, 543.8 nm laser is used as the light source, and two semicircular samples are placed on a goniometer to analyze each of the phenomena described above as the incident angle is changed. The beam is focused into the photodetector by two collimating lenses, and the polarization of the light can be controlled by a polarizer placed before the sample. Before any data is taken, the system is aligned as to have the center of the beam lined up to the center of the detector as closely as possible with the sample and lenses in place.

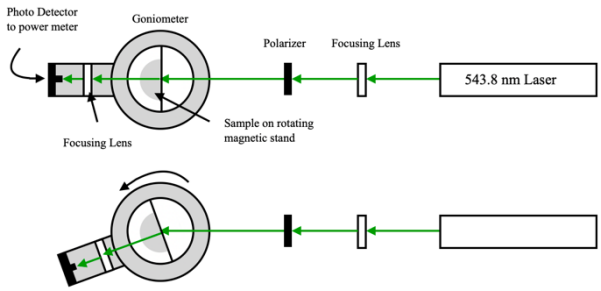

Figure 1: (Top) A schematic of the experimental setup. (Bottom) Example of the sample rotated at some incident angle.

Once everything was aligned, we took preliminary data to determine the critical angle and Brewster's angle. The critical angle could be determined by finding the point where the transmitted beam completely disappeared. However, this situation can only occur when the light passes from the denser medium to the less dense one. Brewster's angle was a little trickier to find, as experimentally there was no angle where the power of the reflected beam equaled zero. Still, there was a point where the reflected beam power was very close to zero, and we used the point where the power was lowest to be Brewster's angle.

To accurately measure the unknown indices of refraction of the materials, both the incident and transmitted beam angles were recorded by using the goniometer and then analyzed with Snell's Law. By plotting data for $\sin(\theta_i)$ vs. $\sin(\theta_t)$, the resulting slope will equal the index of refraction of the material, since the index of refraction of air is approximately equal to 1. This is done for both orientations, material to air as well as air to material, which correspond to the arced side facing the beam and the flat side facing the beam respectively. As previously mentioned, Snell's Law works for both parallel and perpendicular polarizations, so it was sufficient to take data for this part using only one of the two (in our case we used a perpendicular polarization).

Once found, the index of refraction was then used to predict the critical angle of both materials for the material to air transition. This is the only orientation that yields a critical angle since the index of refraction of the materials is greater than that of air, and the argument of arcsine cannot be greater than 1.

Finally, data was then taken to verify the Fresnel equations. The incident beam power was recorded by measuring the laser beam power at 0° without a sample. The initial transmitted power at 0° was also recorded for each scenario

after placing the sample on the stage and setting the polarization configuration. This was done to ensure that our data aligned with the theoretical curves as accurately as possible, it was necessary to incorporate a correction factor into our data for each orientation. This factor arises from the fact that the light is traveling through the sample, so the original incident beam power gets reduced as it travels through the material. Due to the physical system, we needed to adjust our reflectance and transmittance coefficients accordingly:

$$r_{mat\to air} = \frac{I_r}{I_i * T^2(0)}$$
$$t_{mat\to air} = \frac{I_t}{I_i * T(0)}$$
$$r_{air\to mat} = \frac{I_r}{I_i}$$
$$t_{air\to mat} = \frac{I_t}{I_i * T(0)}$$

Here, T(0) represents the transmittance coefficient at zero degrees. Note that the transmittance coefficients are similarly corrected, while the reflectance coefficients differ depending on the orientation. In order to get T(0), we took the power of the transmitted beam at zero degrees (for each corresponding sample and configuration) and divided it by the incident beam power found at zero degrees with no sample.

For a variety of incident angles, the reflected angle, refracted angle, reflected beam power, and transmitted beam power were all recorded. These measurements were taken for both samples at both geometrical orientations and both polarization orientations, to make for eight sets of measurements. In order to get 10-15 different measurements for each set, data was taken every $5°$ starting at $15°$, and going up to as large as $85°$ depending on the phenomena involved[2]. It was difficult to get data at angles smaller than $15°$ since the photodetector screen blocked the incident beam from hitting the sample. While taking data, the reflected angle provided a good way to double check that our system was aligned properly. By the law of reflection, the reflected angle should be equivalent to the incident angle, so a well-aligned system should reflect this.

The reflectance coefficient was plotted using the reflected beam power and the incident beam power measured without a sample in place. The transmittance coefficient was plotted using the transmitted beam power and the same incident beam power. Although the equation calls for the corresponding beam intensities as opposed to beam power, the power is equal to the intensity divided by the area of the beam. In this experiment, the lenses focus the beam so that the photodetector can detect the whole area of the beam, thus, for the most part, making the area a constant. This allows the ratio of powers to be equal to the ratio of intensities.

For each sample, geometrical orientation, and polarization, the incident angle had to be accounted for while measuring the reflected and transmitted angles. This is because the goniometer measures the angles appropriately when the sample is lined up at $0°$ with the rest of the system. However, when the sample is turned $x°$, the incident angle also changes $x°$, and the goniometer does not account for that. Thus, at each angle, the measured reflected angle was larger than the actual reflected angle by the incident angle. When going from a lower to higher index ($n_2 > n_1$), the ray bends towards the surface normal, making the incident angle larger than the transmitted angle, and vice versa. The actual transmitted angle is therefore the measured transmitted angle subtracted from the incident angle for $n_2 > n_1$, and the measured transmitted angle added to the incident angle for $n_1 > n_2$.

There were a few ways in which we accounted for error in this experiment. The first was dealing with the angular error of the goniometer. Since the smallest increment on the goniometer is $1°$, we used $0.5°$ as the error in our angular measurements, adopting standard practice. As for the power measurements, the wattmeter was more erratic, so five measurements were taken at each angle. These were then averaged to find the mean and standard deviation of power at each incident angle. A final thing to mention is that the semicircular samples used in the experiment are not actually perfect semicircles. A consequence of this is that beams leaving the arced side of the sample will not exit exactly perpendicular to the surface, and a slight refraction occurs. We accounted for this by adding in an additional $0.5°$ angular error to the incident and transmitted angles greater than $30°$.

III. DATA AND ANALYSIS

The preliminary results for the critical angle and Brewster's angle of each experimental configuration can be seen below in Table 1. As expected, only the configurations with a P polarization resulted in the appearance of a Brewster's angle, and only the orientations where the laser went from the sample to air interface resulted in the appearance of a critical angle. We were also able to distinguish between Brewster's angle and the critical angle because the critical angle was the same regardless of the beam polarization. Once it was found

[2] For example, a specific orientation may have had more data points taken around Brewster's angle or the critical angle and less around the larger angles.

for the S polarization, then we knew that we were looking at the critical angle and not the Brewster angle.

Preliminary Findings			
Interface	**Polarization**	**Brewster's Angle**	**Critical Angle**
Glass → Air	S	--	41°
Glass → Air	P	34°	42°
Air → Glass	S	--	--
Air → Glass	P	58°	--
Plastic → Air	S	--	41°
Plastic → Air	P	32°	41°
Air → Plastic	S	--	--
Air → Plastic	P	55°	--

Table 1: Preliminary results for the critical angle and Brewster's angle for each of the 8 possible configurations.

The results for our analysis of the indices of refraction of the two materials using Snell's Law can be seen below in Figure 2. The data was analyzed in Python and a line of best fit was made using a fitting package, which was able to account for the angular errors. The sines of each angle were plotted, and their ratio is equal to the index of refraction of the material in question.

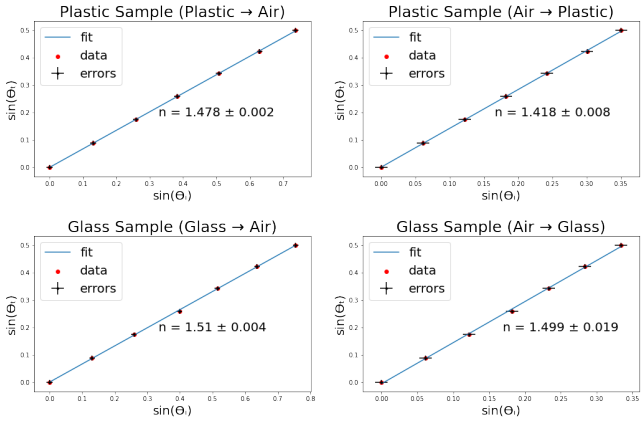

Figure 2: Transmitted angle as a function of the incident angle for the two samples, each looked at for the two medium transitions. A line of best fit was made from the collected data and their respective errors.

Each calculated index of refraction falls within what is expected for the corresponding material (based off of results found in [6] for the wavelength of laser light used). As a further comfort, each orientation yields approximately the same index of refraction as the other for a given material. Theoretically, we expect that the calculated index of refraction should be independent of the orientation of the sample, and each will yield the same exact value. This is because Snell's Law describes the behavior of light at a boundary regardless of the orientation, and if the directions are reversed the numerical values should remain the same. It can be seen that the two calculated indices for the glass sample are very close to each other, only off by 0.012, which is small considering the setup used (~.85% relative error). As for the plastic samples, their values disagree by 0.06, which is 5 times more that the glass disagreement, however this value is still relatively small (~4% relative error). The discrepancies seen in our results can be explained due to a few factors. It is possible that there were slight misalignments of the sample on the stage, which causes the incident and transmitted angles to be slightly off. The initial alignment is made especially difficult due to the imperfect shape of the sample. Even if one sample is lined up perfectly, we cannot just rotate it 180° to then be perfectly aligned in the other orientation. It required us to re-place the sample on the stage and try to find the center again. The fact that the plastic sample was much smaller than the glass sample may have also caused further discrepancies, as it was more difficult to tell when the sample was directly on the center of the goniometer.

The results of measuring the reflectance and transmittance as a function of the incident angle for the glass and plastic samples can be seen in Figure 3 and Figure 4 respectively.

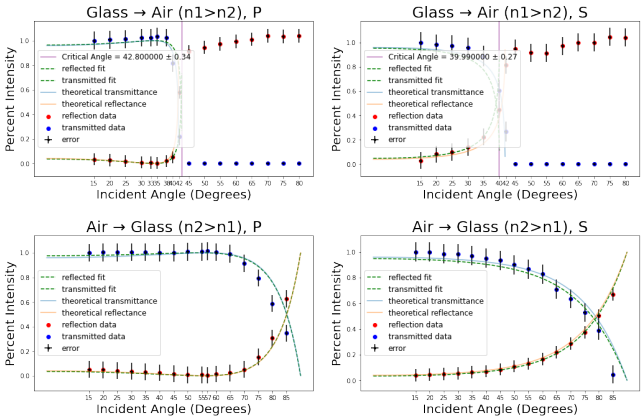

Figure 3: Reflectance and transmittance coefficients were plotted as a function of the incident angle for the 4 glass configurations alongside theoretical expectations and a fit of the data.

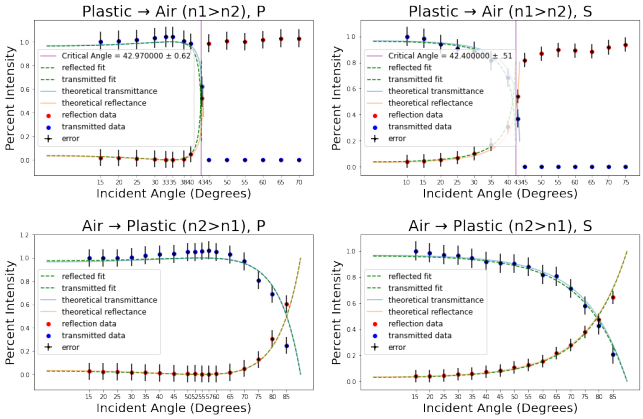

Figure 4: Reflectance and transmittance coefficients were plotted as a function of the incident angle for the 4 plastic configurations alongside theoretical expectations and a fit of the data.

For both samples, we can see that our reflectance and transmittance data points line up nicely against the theoretical curves. In each configuration, the theoretical curve not only follows a similar shape to our data, but it also falls mostly within or close to our error bars. It is also important to note that at any given angle, the two values sum to 1 as expected for any of the configurations. Our data also behaves predictably in regard to Brewster's angle and the critical angle. Brewster's angle can be seen in each P polarization case by the dip in the reflectance curve (as well as the corresponding raise in the transmittance curve). The critical angle is also apparent in cases where the laser beam went from sample to air by an abrupt drop in the transmittance curve. After the critical angle, all remaining incident angles yield zero for the transmittance coefficient and about one for the reflectance coefficient.

Figure 5 below shows a zoom in on the Brewster's angle for each experimental configuration with a P polarization, along with a line of best fit to calculate the experimentally determined value.

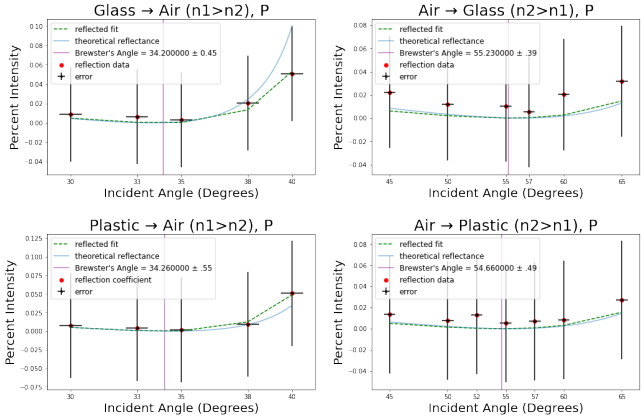

Figure 5: Zoom in on the Brewster's angle of each P polarization

After zooming in on the dip of each reflectance curve, the data was fitted so that Brewster's angle could be found at the minimum of the fit. In Table 2 below, the Brewster's angles found from the fit are compared to angles calculated using the experimentally found indices of refraction. The values from the fit are all within a 3% error of our predicted values calculated from the indices of refraction, showing agreement between the two different methods. The slight discrepancies arise from the different methodology used to determine the values, one using angles and the other power measurements.

Brewster's Angle via Different Methods			
Interface	**Polarization**	$\boldsymbol{\theta_b = \arctan\left(\frac{n_2}{n_1}\right)}$	$\boldsymbol{\theta_b}$ **From Fit**
Glass → Air	P	34.59°	34.20°
Air → Glass	P	55.41°	55.23°
Plastic → Air	P	33.69°	34.26°
Air → Plastic	P	56.31°	54.66°

Table 2: Comparison of Brewster's angle calculated theoretically and from a fit of the data.

Index of Refraction (Glass) via Different Methods			
Configuration	$\boldsymbol{\theta_b}$ **From Fit**	$\boldsymbol{\theta_c}$ **From Fit**	**n**
Glass → Air, P	34.20°		1.45
Air → Glass, P	55.23°		1.44
Glass → Air, P		42.80°	1.47
Glass → Air, S		40.00°	1.56
			Avg: 1.48
			Snell's: 1.50
Index of Refraction (Plastic) via Different Methods			
Configuration	$\boldsymbol{\theta_b}$ **From Fit**	$\boldsymbol{\theta_c}$ **From Fit**	**n**
Plastic → Air, P	34.26°		1.47
Air → Plastic, P	54.66°		1.41
Plastic → Air, P		42.97°	1.47
Plastic → Air, S		42.40°	1.48
			Avg: 1.46
			Snell's: 1.45

Table 3: Comparison of indices of refraction calculated using different methods. For each sample, the first two calculations for n used the Brewster's angles found from fits, while the second two used the critical angles. The average of these four values was taken and compared to the value of n found from Snell's Law earlier in the experiment.

Finally, the Brewster's angles and critical angles found from the data were used to calculate the index of refraction for each sample. This was done by putting the angle values into the equations for Brewster's angle and critical angle, and solving for the proper index of refraction, knowing that the index of refraction for air is 1. Table 3 shows these calculated values compared with the original experimental values discovered in the beginning of the experiment. While comparing the average of the indices of refraction calculated from the fits against the Snell's Law calculation, the index of refraction for glass differed by 1.3%, while that of plastic differed by 0.7%. These statistics verify that our data is reliable and consistent, and that the Fresnel equations accurately describe the behavior of light at a boundary.

IV. CONCLUSION

From our experimental findings, we conclude that Snell's Law and the Fresnel equations accurately describe the phenomena that occurs for light between two different media. Our data agrees well with the theoretical curves within its error bars and each experimental configuration yielded answers we expected to see (e.g. the index of refraction for the same material being approximately the same regardless of orientation). We can account for places where the theoretical curve doesn't fall within our error bounds by experimental error. One factor of this error, as mentioned before, is the fact that the samples we used were not perfect semi-circles. Another source of error came from the photodetector. While the beam is aimed at the hole at the front, the actual photodetector sits behind the hole, so it is difficult to verify the detector is capturing the entire area of the beam. We feel as though this experiment could definitely be improved with a better setup. Unfortunately, most of the optics used in the experiment were easy to move and this

allowed for frequent misalignments of the beam. This was especially true for the laser used, as it was not even attached to the same system that the optics were a part of (the Pasco track). If the setup was to be screwed into an optics table, it would allow for minimal movement and would certainly help to minimize error accumulated during the experiment.

V. REFERENECES

[1] Phillip Rechani, Phil's E&M, https://drive.google.com/file/d/15J8vG1liDpWOoN8gGnkLg-Ucpv3pStJ7/view.

[2] D. J. Griffiths, Introduction to Electrodynamics, 3rd ed., Prentice Hall, Upper Saddle River 1999.

[3] Mikhail Polyanskiy, Refractive Index Database, https://refractiveindex.info/.

VI. APPENDIX

Raw data gather from our experiment can be found the tables below.

Glass Sample			
Enter Semicircle side		Enter Flat side	
Incident Angle (degrees)	Transmitted Angle (degrees)	Incident Angle (degrees)	Transmitted Angle (degrees)
0	0	0	0
5	7.5	5	3.5
10	15	10	7
15	22.5	15	10.5
20	30.5	20	14
25	39	25	17.5
30	47.5	30	20.5

Table 3: Raw data for measuring the index of refraction with Snell's Law of the glass sample. Data was taken for both orientations.

Plastic Sample			
Enter Semicircle side		Enter Flat side	
Incident Angle (degrees)	Transmitted Angle (degrees)	Incident Angle (degrees)	Transmitted Angle (degrees)
0	0	0	0
5	7.5	5	3.5
10	15	10	7
15	23.5	15	10.5
20	31	20	13.5
25	39.5	25	16.5
30	49	30	19.5

Table 4: Raw data for measuring the index of refraction with Snell's Law of the plastic sample. Data was taken for both orientations.

Glass --> Air (n1>n2), S polarization				
PREDICTION: Brewsters = none, Critical = 42.6°				
θ_i (°)	θ_r corrected (°)	θ_t corrected (°)	P_r (μW)	P_t (μW)
15	13	21.5	2.066	122.2
20	20	30	5.774	120
25	25	39	7.05	119
30	29.5	47	9.932	116.8
35	34	59	15.88	108.6
40	39	72.5	31.94	74.12
42	44	83	58	33
45	44		67.56	0
50	49		65.14	0
55	54		64.9	0
60	59		69.16	0
65	63		71.2	0
70	69		71.2	0
75	73		74.4	0
80	79		74	0

Table 5: Raw angular and power data taken for Glass to Air orientation with S Polarization.

Air --> **Glass** (n2>n1), S polarization				
PREDICTION: Brewsters = none, Critical = none				
θ_i (°)	θ_r corrected (°)	θ_t corrected (°)	P_r (μW)	P_t (μW)
15	15	9.5	8.602	139
20	20	13	9.146	139
25	26	15	10.12	137
30	31	19	11.48	137
35	37	21	13.6	135
40	40	24	15	132.4
45	46	27	18	129.8
50	52	30	23.06	125.2
55	56	32.5	27.22	120.4
60	62	35	35.08	115.2
65	66.5	36.5	45.98	98.76
70	72	37	60.12	88.58
75	76	38.5	78.76	73.62
80	81	37.5	106.4	54.02
85	86	38.5	140.8	6.516

Table 6: Raw angular and power data taken for Air to Glass orientation with S Polarization.

Air --> **Glass** (n2>n1), P polarization				
PREDICTION: Brewsters = 57.8°, Critical = none				
θ_i (°)	θ_r corrected (°)	θ_t corrected (°)	P_r (μW)	P_t (μW)
15	15	20	7.582	148.2
20	20	27.5	7.086	148.6
25	25	34	6.142	148.6
30	30	40.5	5.346	148.8
35	35	47	4.624	148.8
40	40	55	3.576	148.4
45	47	62	2.328	148.2
50	50	69	1.214	149.4
55	54	77.5	1.08	149.4
57	67	83	0.548	150.2
60	60	89	2.112	149.2
65	65	96	3.3	147
70	70	102	7.688	135.4
75	75	112	22.62	117.8
80	81	121	45.38	87
85	86	132	92.72	51.4

Table 7: Raw angular and power data taken for Air to Glass orientation with P Polarization.

Glass --> Air (n1>n2), P polarization				
PREDICTION: Brewsters = 32.17°, Critical = 42.6°				
θ_i (°)	θ_r corrected (°)	θ_t corrected (°)	P_r (μW)	P_t (μW)
15	14	25	3.43	146.6
20	19.5	32	2.788	147.6
25	23	41	1.938	148.4
30	28	50.5	0.8854	150
33	33	56	0.645	150
35	34	63	0.286	151.2
38	36	68	2.086	150
40	39	86	5.182	119.6
42	42	93	59	32
45	43		93.2	0
50	48		96.72	0
55	54		99.66	0
60	59		101.6	0
65	63		103.4	0
70	69		106.2	0
75	73		105.8	0
80	78		106.4	0

Table 8: Raw angular and power data taken for Glass to Air orientation with P Polarization.

Air --> **Plastic** (n2>n1), S polarization				
PREDICTION: Brewsters = none, Critical = none				
θ_i (°)	θ_r corrected (°)	θ_t corrected (°)	P_r (μW)	P_t (μW)
15	15	10	7.994	143
20	20	12.5	8.798	140.8
25	25	16	9.814	138.8
30	30.5	19.5	11.14	138.2
35	35.5	22	12.84	135
40	40.5	25	15.26	131.4
45	45	27.5	17.88	129.6
50	50.5	30	22.2	129.2
55	55	32.5	26.86	125.8
60	60.5	35	32.12	117.2
65	65	36	45.52	115.2
70	70.5	38	58.44	102.12
75	75.5	39.5	79.54	83.1
80	80.5	40	99.72	61.28
85	84.5	41	135.2	29.34

Table 9: Raw angular and power data taken for Air to Plastic orientation with S Polarization.

Plastic --> Air (n1>n2), P polarization				
PREDICTION: Brewsters = 34.59°, Critical = 41.5°				
θ_i (°)	θ_r corrected (°)	θ_t corrected (°)	P_r (μW)	P_t (μW)
15	15	22.5	1.34	122
20	20	30	1.24	123
25	25	38	0.97	124
30	30	47	0.53	126
33	32	54	0.27	127
35	35	58	0.1	127
38	37	65.5	0.65	123
40	40	70.5	3.6	120
43	43	81	37	76
45	45		70	0
50	50		71.5	0
55	55		71	0
60	60		72	0
65	65		73	0
70	70		73	0

Table 10: Raw angular and power data taken for Plastic to Air orientation with P Polarization.

Air --> **Plastic** (n2>n1), P polarization				
PREDICTION: Brewsters = 55.41°, Critical = none				
θ_i (°)	θ_r corrected (°)	θ_t corrected (°)	P_r (μW)	P_t (μW)
15	15	10.5	3.73	137
20	20	14	3.54	137
25	25	17	3.16	137
30	30	20	2.71	138
35	35	23	2.22	140
40	40	25.5	1.72	141
45	45	29	1.23	142
50	50	31.5	0.69	144
52.5	52.5	36	1.16	144
55	55	34.5	0.459	145
57.5	57.5	39	0.63	146
60	60	37	0.75	144
65	65	39	2.41	141
70	70	40	7.19	133
75	75	42.5	17.6	111
80	80	44	42	94.5
85	85	45	83	34.2

Table 11: Raw angular and power data taken for Air to Plastic orientation with P Polarization.

Plastic --> Air (n1>n2), S polarization				
PREDICTION: Brewsters = none, Critical = 41.5°				
θ_i (°)	θ_r corrected (°)	θ_t corrected (°)	P_r (μW)	P_t (μW)
10	10	15.5	3.962	143.6
15	15	23.5	4.304	141.6
20	20	32	5.268	135.2
25	25.5	41	6.842	130.2
30	30	50	9.908	127.6
35	35	61	16.72	117
40	40	78.5	29.86	98.2
43	39	89	53.02	53.2
45	45		80.4	0
50	50		85.2	0
55	55		88.1	0
60	60		87.5	0
65	65		86.8	0
70	70		90	0
75	75		92	0

Table 12: Raw angular and power data taken for Plastic to Air orientation with S Polarization.